Design, Implementation and Comparison of Several Neural Perturb and Observe MPPT Methods for Photovoltaic Systems

Ihssane Chtouki*‡, Patrice Wira**, Malika Zazi*, Bruno Collicchio**,Sami Meddour***

*Department of Electrical Engineering, ERERA Research Team, ENSET, Mohammed V University, Avenue des Nations Unies,10102 Rabat,Morocco

** Institute of Research in Computer Science, Mathematics, Automation and Signal, Haute Alsace University, 61 rue Albert Camus, 68093 Mulhouse, France

***Laboratory of Electrical Engineering and Automatic (LGEA) Larbi Ben M'hidi University Oum El Bouaghi, Algeria.

‡ Corresponding Author, Chtouki ihssane, Department of Electrical Engineering, ERERA Research Team, ENSET, Mohammed V University Avenue des Nations Unies,10102 Rabat,Morocco, Tel: +33 755896334, Ihssane.chtouki@gmail.com

Received: 19.03.2019 Accepted:10.05.2019

Abstract- The present article describe several Genetic Algorithms (GAs) neural controllers MPPT strategies that used to apply to a voltage step-up converter driven by a PV stand-alone system. A new kind of control structures based on different input variables, combined to three categories of techniques to develop an adaptive MPPT approach: the Perturb and Observe (P&O) technique is associated to a Multilayer Perceptron (MLP) using GAs as learning suggestion abilities. It is used in order to optimize the controller efficiency by driving the network through the use of new information in synaptic connections to get an optimal learning rule whatever the changing weather and load conditions. Based on environmental sensors an experimental data has been collected to settle the learning sets for the learning algorithm of the MLP. In consequence, the performances of the proposed GA neural controllers inserted in a complete MPPT strategy have been validated with simulation tests using the Matlab/Simulink environment. Good result has been confirmed and compared inside a test bench based on real PV system with boost converter and resistive load piloted by the dSpace 1104 card. The superior characteristics of the electrical structure using GAs neural controller is affirmed in terms of performance assessment covers overshoot 20%, robustness, transient/steady-state performance, time response 0.05s, and oscillations < 10^{-4}.

Keywords: Photovoltaic system, solar energy, P&O, artificial neural network, GA, dSpace 1104.

Nomenclature

I_{Pv}	is the PVcurrent module	G_{Smc}	is the nominal solar radiation at standard conditions
I_{Ph}	is the is photocurrent PV module	$W_{i,j}$	the synaptic weights
$I_{s,Smc}$	the reverse saturation current	B_j	is the bias
$I_{sc,smc}$	the short circuit current per cell	$\propto_{optim}$	is the optimal control value
I_s	the saturation current of the PV cell	^{H}	Hidden layer
V_t	is the thermal voltage of the cell	^{IH}	Input to hidden layer
n	is the diode ideality factor	σ	The sigmoid activation function
k	is the Boltzmann's constant (1.3806503 10-23 J/K)	^{HO}	Hidden to output lay
V	is the voltage of the diode	e	error for the Kth exemplary
q	is the charge of an electron (q= 1.610-19 C)	e_k	error for the kth exemplary
k_i	is the current coefficient	λ	is a default learning parameter
k_v	is the Voltage c	I	is the matrix of identity
V_{oc}	is the open circuit voltage at the nominal condition	G	is the solar radiation on the device surface

1. Introduction

The amount of energy generated from a photovoltaic installation depends mainly on the following factors: temperature and solar irradiance. It is convenient to operate at the point of maximum power (MPP) which changes with the solar luminous intensity, or with load variations. These have a complex relationship between all this parameter which produces a "Current – Voltage" curve with a characteristic of a non-linear output. The problem is how to obtain optimum operating points (voltage and current) to maximize output photovoltaic power whatever the variations of the weather conditions. Numerous MPPT techniques have been developed for photovoltaic system such as Hill Climbing (HC), Incremental Conductance (IC), [1] Perturb and Observe (P&O), Constant Voltage (CV), Short-Current (SC) and [2,3] open circuit (Open Voltage), Parasitic Capacitance (PC) and Neural Networks (NNs), [4,5] fuzzy logic control (FL). More recently, we have found that techniques based on [6] Evolutionary algorithms. (Artificial Neural Networks) (ANNs) [7] are an efficient nonlinear training techniques; this means that the data-based approaches that lead to the development of independent to adaptive systems [7]. ANNs [8, 9] can detect the nonlinear multiple interactions among a variety of variables and can therefore handle complex relationships between two reference frames. In the context of optimization, this work describes ANN controllers with GAs used to achieve an improved MPPT strategy. GAs belongs to the family of evolutionary algorithms [6, 10]; in this article it is used to optimize MLP neural networks weights [10] thanks to a chromosome representation. The idea consists in learning, designing and implementing in real time an ANN inspired from nature and evolution based on GAs. The goal of this GA-based neural control is to maximize power extraction under all conditions. Indeed, the control of the energy conversion must be adaptive in order to respond in real- time, as well as to draw as much power as possible through a solar panel under all charging conditions (load and weather conditions). Three neural proposed structures using GAs strategy to reduce an error function [11] derived from a self-associative neural network, their originality consists in the type of their structures and input variables chosen, which can be either electrical, environmental or hybrid parameters. The first GA based neural controller takes the variation of the power and the variation of the panel voltage as inputs represents a way to predict the next value of the power and provides the instantaneous value of the duty cycle. The second GA based neural controller uses two inputs: The irradiation and the panel current the output is the power expected given by the duty cycle (α) to monitor the boost converter. This controller combines electrical parameters and weather information (irradiance) from additional sensors to optimize the energy conversion. The third GA based neural controller requires the irradiation and the temperature (as the inputs) to provide the value of the duty cycle (one output). As expected, we have implemented GA based ANN techniques as an easy alternative to improve the performances to one of the most important popular MPPT technique, the P&O method. The principal motivations are the followings: With GAs based learning abilities the P&O MPPT algorithm will be dedicated to specific PV panels and will be adaptive to changing conditions. As a consequence, the answers obtained with the learning approach are good, i.e., faster and more efficient in the power conversion. This allows overcoming the problems of the conventional P&O method, i.e., oscillations surroundings the MPP, and its low follow-up response in rapidly and slowly changing meteorological conditions, despite the worst cases. The benefits of being used ANNs in conjunction with GAs are their capacity to handle a variety of non-linearities, and to treat problems with no prior knowledge, that is, to use no intern model. The resolution of the problem of learning neural networks by evolutionary algorithms shows that GAs converges toward global optimum. This article is about developing and implementing a complete solar photovoltaic conversion chain of medium power (145W). Two electrical structures based GA neural controller and Levenberg-Marquardt (LM)[15] algorithm are compared and implemented via DS1104 card inside a real test bench using boost- converter and variable resistance as shown in Fig1., as a results the GA learning approach confirmed that the high electrical performances in function of rapidity, accuracy and oscillations has two goals: Predict PV array power output and quickly track MPP by setting weights from a MLP to a GA strategy whatever the variations of weather conditions.

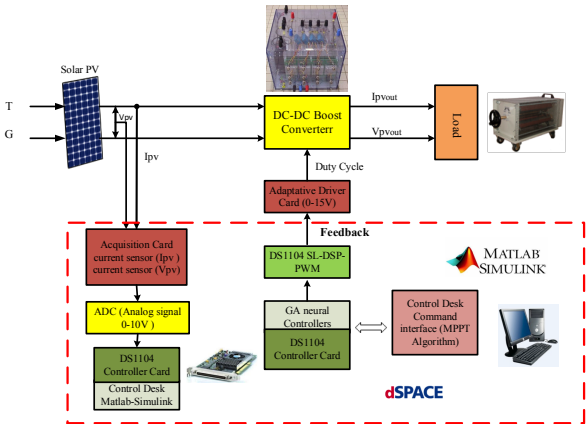

Fig. 1. The complete PV conversion implemented system.

2. PV Model Connected through a DC/DC Boost Converter

2.1. PV cell mathematical modelling using Newton Raphson (N-R)

This part present an electronic solar cell circuit used to emulate the operations of Photovoltaic (PV) cell. Based on a datasheet of real PV panel presented by table 2 of system parameters, and on mathematical linearized equations of N-R [12]. The PV is modelled using Power system Toolbox [13] of Matlab /Simulink.

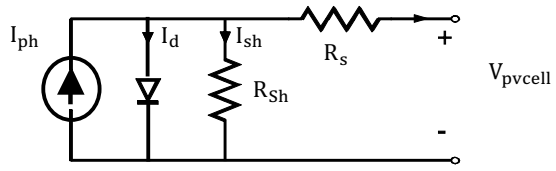

Fig.2. Model of a photovoltaic cell.

Using the Kirchhoff law, the current I is given by:

$$I_{pv} = I_{ph} - I_d - I_{Sh} \quad (1)$$

$$I_{pv} = I_{ph} - I_s\left[\exp\left(\frac{v + IR_s}{v_t n}\right) - 1\right] - \frac{v + IR_s}{R_p} \quad (2)$$

With $$a = \frac{n.K.T_{Smc}}{q} = n.v_t \quad (3)$$

$$v_t = \frac{KT_{Smc}}{q} \quad (4)$$

The relation between the photocurrent PV module, solar radiation, the temperature and the short circuit current are given by:

$$I_{ph} = \left(I_{Sc,Smc} + K_i \Delta T\right)\frac{G}{G_{Smc}} \quad (5)$$

The reverse saturation current is given by

$$I_{S,Smc} = \frac{I_{Sc,Smc}}{\left[\exp\left(\frac{qV_{oc}}{KnT_{Smc}}\right) - 1\right]} \quad (6)$$

The saturation current of the PV cell depends on the cell temperature given by:

$$I_S = I_{S,Smc}\left[\left(\frac{T_c}{T_{Smc}}\right)^3 \exp\left(\frac{qE_G\left(\frac{1}{TSmc} - \frac{1}{Tc}\right)}{Kn}\right)\right] \quad (7)$$

Using an iterative method, N-R is used to solve the non-linearity of the equation current (2). The N-R technique requires the function which has a tangent in each of the points of the sequence that one builds by iteration, for example it is enough that f is differentiable. Starting from a point x_0 that we choose preferably close to zero the function f(x) using a Taylor series expansion in $(x\text{-}x_0)$ is giving by:

$$f(x) = f(x_0) + f'(x_0)(x - x_0) + 1/2 f''(x_0)(x - x_0)^2 + \ldots = 0 \quad (8)$$

$$X_{K+1} = X_K - \frac{f(x_K)}{f'(x_K)} \quad (9)$$

On the curve I-V we found three operation areas of photovoltaic generator, short-circuit condition, maximum power-point condition and open-circuit condition. For the open-circuit condition we have (I=0 and V = V_0), by introducing this conditions in equation (2) we get:

$$I_{ph} = I_s\left(\exp\left[\frac{V_0}{av_t}\right] - 1\right) - \frac{V_0}{R_p} \quad (10)$$

The derivative of the equation (2) is giving by [12]:

$$\frac{dI}{dV} = -I_S\left(\frac{1}{V_t}\left(1 + \frac{dI}{dV}R_s\right)\exp\left[\frac{V + IR_s}{nV_t}\right]\right) - \frac{1}{R_p}\left(1 + \frac{dI}{dV}R_s\right) \quad (11)$$

By introducing short-circuit condition in equation (11) we obtain:

$$\left[\frac{dI}{dV}\right]_{I=1} = I_S\left\{\frac{1}{V_t}\left(1 + \left[\frac{dI}{dV}\right]_{I=1}R_s\right)\exp\left[\frac{V_0}{nV_t}\right]\right\}\frac{1}{R_p}\left(1 + \left[\frac{dI}{dV}\right]_{I=1}R_s\right) \quad (12)$$

As a result the equation (12) is easily solved in Matlab. This circuit emulates the dynamic characteristics of our PV model in SMC Fig.3. And regarding to the changes of weather conditions (irradiation and temperature) Fig.4.

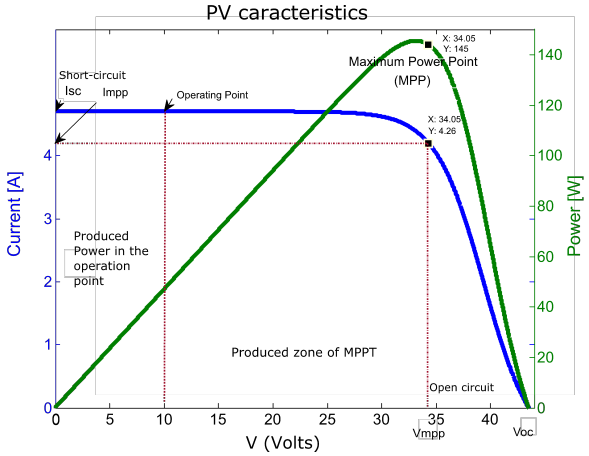

Fig. 3. The dynamics operation of PV cell at standard condition using Matlab

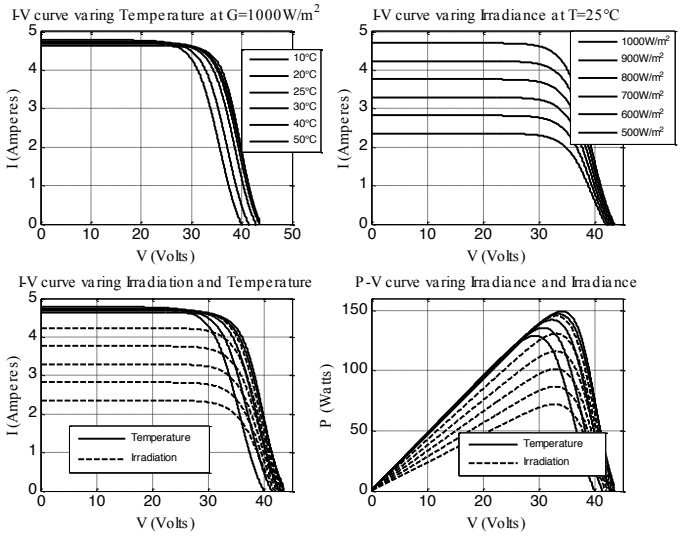

Fig. 4. The dynamics characteristics of PV system (I, P, V) using Matlab.

2.2 Interconnected standalone PV system using DC/DC boost converter

A boost is a voltage elevator converter of the DC-DC type, in our application acts as an interface between the solar panel and the supplied resistive load. The equivalent circuit model simulated is given by Fig. 5 using Matlab/Simulink. The switch S1, symbolized here as a power MOSFET, is rendered conductive periodically with a duty cycle α.

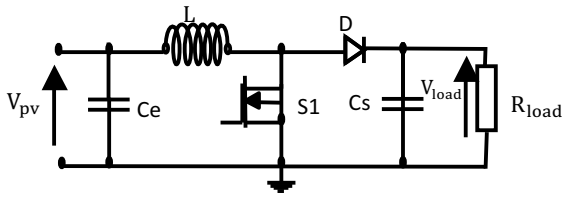

Fig. 5. DC-DC Boost converter

The relation between the boost's input and output signal voltage [14] is:

$$\frac{V_{load}}{Vpv} = \frac{1}{1-\alpha} \qquad (13)$$

The sizing of the boost parameters is based on the inductance L, the switching frequency f_s, and the output capacitor C:

$$C = \frac{Vbus\max}{4.fs.\Delta I_e} \qquad (14)$$

$$L = \frac{Vbus\max}{4.f_s.\Delta I_e} = \frac{2V_{pv}}{4.f_s.\Delta I_e} \qquad (15)$$

The calculate parameters are found in table 1.

3. Proposed Neural Control Techniques for PV System

MLP are the most well known neural networks used in identification and control, a perceptron is a network of artificial neurons of the "Feedforward" type. Among the problems of the use of MLP consists in the choice of its architecture. In the literature, there is a large amount of more sophisticated learning algorithms, some of which can be mentioned: Descending Gradient with Variable Learning Rate; Resilient retropropagation; the conjugate gradient algorithm; The Fletcher-Reeves algorithm; Quasi-Newton Algorithm; LM [15] Algorithm. Among this entire algorithm, LM is the best used one. However, for some very regular functions, it can converge slightly slower. For the problems of approximation of functions where the number of the weights of the network is less than one hundred. When the number of weights increases the effectiveness of the LM algorithm decreases, as well as this algorithm is poor for optimization function problems. In this work, we applied a GA technique [16] to optimize the parameters of MLP neural networks in order to enhance its accuracy. The study proposes three different structures ANNs with different types of input measures. Whatever the configuration, the ANN always outputs α. The error of each structure is adapted automatically using GA, the best structure is implemented in real time and compared with the same one trained with LM algorithm. The objective is to find out an enhanced MPPT method for pv system.

3.1 GA used to train Artificial Neural Network for PV MPPT system architectures

Three schemes have been proposed in this paper to model the control of the MPPT PV system given in Figures 6, 7, 8 using different input variables are presented based in [17]: Electrical which take the power variation and voltage variation, Environmental which include temperature and irradiation and hydride which take the irradiation and current. In addition, an output value of the duty cycle is provided to drive the MPP solar PV.

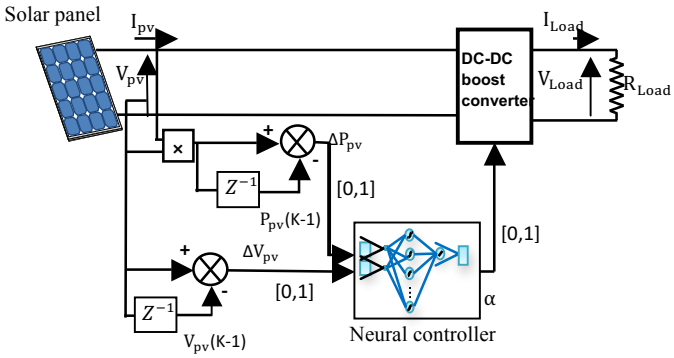

Fig. 6. Neural P&O controller using electrical input parameters

The purpose of this part is to solve the problem of the optimization of the photovoltaic system, and to find the optimal control (α) for the boost converter. The weight and bias in this application are optimized by the GA learning approach so that the network solves the problem. The variations of MPP are in function of temperature and irradiation; build a database of neural network learning. The inputs are the parameters collected by the environment using sensors and by simulation on the Matlab environment, the network output is the control to maximize the output power of the solar PV.

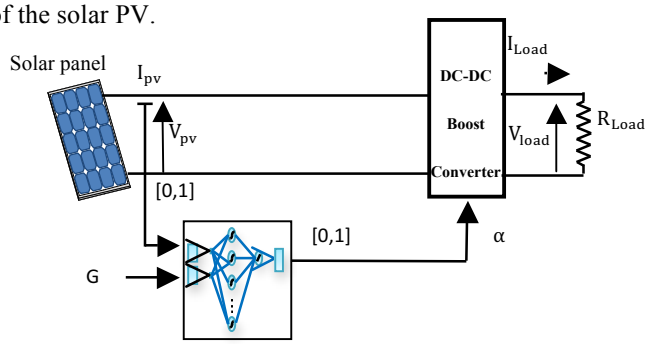

Fig. 7. Neural P&O controller using electrical and environmental input parameters.

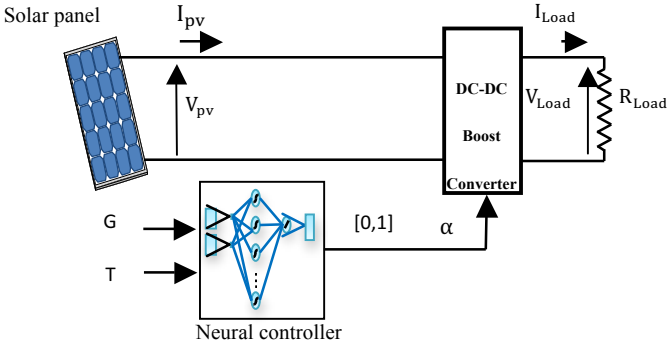

Fig.8. Neural (P&O) controller using environmental input parameters

Variations of MPP in function of temperature and irradiation have been built to a database of neural network learning. The objective function used in this work to solve the problem is depending on the nature of the inputs of NNs, especially depending on the synaptic weight of neurons. We can write it under 2 forms:

$$F=\begin{cases}\propto (X_i, W_{i,j}, B_j) / \propto_{optim} \\ \text{if} \quad \propto_{optim} > \propto\end{cases}$$

With X_i is the inputs: (ΔV_{pv}, ΔP_{pv}, T, G, I_{pv}).

The maximization problem is subject to the following inequality constraints [7]:

$$F(c)=\frac{1}{error}=\frac{1}{\alpha-\alpha_{optim}}>0 \qquad \alpha_{optim}>\alpha \tag{16}$$

The mean square error is giving by:

With $$E=\frac{1}{2}\left(desired-\frac{1}{1+e^{-\alpha_{optim}}}\right)^2 \tag{17}$$

The ANN used in this article is composed of: 2 neurons in the input layer, 10 neurons in the hidden layer and one neuron in the output layer. Using this structure we can calculate the parameters of the NNs [7] using the following equation:

$$\exists(i,j), i\neq j \; H_{i,j}=\sigma\left(B_i^{H}+W_{i,j}^{IH}.X_j\right) \; i>j \tag{18}$$

With $i>j$ i: is the number of neurons in the hidden layer.

j: is the number of neurons in the input layer .

$$H_{10,2}=\sigma\left(B_{10}^{H}+W_{10,2}^{IH}.X_2\right) \tag{19}$$

The output NNs can be calculated using the following equations:

$$\alpha_{1,10}=\sigma\left(B_1^{O}+W_{1,10}^{HO}.\mathrm{H}_{10,2}\right) \tag{20}$$

$$\alpha_{optim}=\sigma\left(B_1^{O}+W_{1,10}^{HO}.H_{10,2}\right) \tag{21}$$

The matrix representations of the control [7] developing in (21) are giving by:

$$\alpha_{optim}=\sigma B_1^{O}+\begin{bmatrix}\sigma W_{1,1}^{HO}\\ \sigma W_{2,1}^{HO}\\ \sigma W_{3,1}^{HO}\\ \sigma W_{4,1}^{HO}\\ \sigma W_{5,1}^{HO}\\ \sigma W_{6,1}^{HO}\\ \sigma W_{7,1}^{HO}\\ \sigma W_{8,1}^{HO}\\ \sigma W_{9,1}^{HO}\\ \sigma W_{10,1}^{HO}\end{bmatrix}.H_{10,2} \tag{22}$$

$$H_{10,2}=\begin{bmatrix}\sigma W_{1,1}^{H}X_1+\sigma W_{1,2}^{H}X_2+\sigma B_1^{H}\\ \sigma W_{2,1}^{H}X_1+\sigma W_{2,2}^{H}X_2+\sigma B_2^{H}\\ \sigma W_{3,1}^{H}X_1+\sigma W_{3,2}^{H}X_2+\sigma B_3^{H}\\ \sigma W_{4,1}^{H}X_1+\sigma W_{4,2}^{H}X_2+\sigma B_4^{H}\\ \sigma W_{5,1}^{H}X_1+\sigma W_{5,2}^{H}X_2+\sigma B_5^{H}\\ \sigma W_{6,1}^{H}X_1+\sigma W_{6,2}^{H}X_2+\sigma B_6^{H}\\ \sigma W_{7,1}^{H}X_1+\sigma W_{7,2}^{H}X_2+\sigma B_7^{H}\\ \sigma W_{8,1}^{H}X_1+\sigma W_{8,2}^{H}X_2+\sigma B_8^{H}\\ \sigma W_{9,1}^{H}X_1+\sigma W_{9,2}^{H}X_2+\sigma B_9^{H}\\ \sigma W_{10,1}^{H}X_1+\sigma W_{10,2}^{H}X_2+\sigma B_{10}^{H}\end{bmatrix} \tag{23}$$

With X_1, X_2 are the inputs of the three proposed configurations fig (6,7,8), ((ΔV_{pv}, ΔP_{pv}); (G, I_{pv}); (G, T)) that will be optimizing to maximize power in output Pv the control applied to the converter for each structure is giving by the following equations:

$$\alpha_{\Delta V_{pv},\Delta P_{pv}}=\sigma\left(B_1^{O}+W_{1,10}^{HO}.\sigma\left(B_{10}^{H}+W_{10.2}^{IH}.X_{\Delta V_{pv},\Delta P_{pv}}\right)\right) \tag{24}$$

$$\alpha_{G,I_{pv}}=\sigma\left(B_1^{O}+W_{1,10}^{HO}.\sigma\left(B_{10}^{H}+W_{10.2}^{IH}.X_{G,I_{pv}}\right)\right) \tag{25}$$

$$\alpha_{G,T}=\sigma\left(B_1^{O}+W_{1,10}^{HO}.\sigma\left(B_{10}^{H}+W_{10.2}^{IH}.X_{G,T}\right)\right) \tag{26}$$

To replay to the condition of the objective function we have:

$$\sigma=F(X)=\frac{1}{1+e^{-x}} \tag{27}$$

By remplacing (21) in (28) we have:

$$F\left(\alpha_{optim}\right)=\frac{1}{1+e^{-\alpha_{optim}}} \tag{28}$$

$$F\left(\alpha_{optim}\right)=\frac{1}{1+e^{-\left(B_1+W_{1,10}\cdot\frac{1}{1+e^{-(B_{10}+W_{10,2}\cdot X_2)}}\right)}} \tag{29}$$

Where the error is

$$E=\frac{1}{2}\left(desired-\frac{1}{1+e^{-\left(B_1+W_{1,10}\cdot\frac{1}{1+e^{-(B_{10}+W_{10,2}\cdot X_2)}}\right)}}\right)^2 \tag{30}$$

The general principle of the (GA)[11][18] technique is explained by Fig.6. The algorithm starts from an arbitrary population of randomly selected potential solutions (chromosomes). Their relative performance (fitness) is assessed. Based on these performances, a new population of potential solutions is created by using simple scalable operators: Selection, crossing and mutation. This process is repeated until a satisfying solution is achieved. In practical terms, this algorithm achieves a good job by including an" objective function" or" error function"[16]. Here, the criterion of the mean square error (MSE) is used as an objective function:

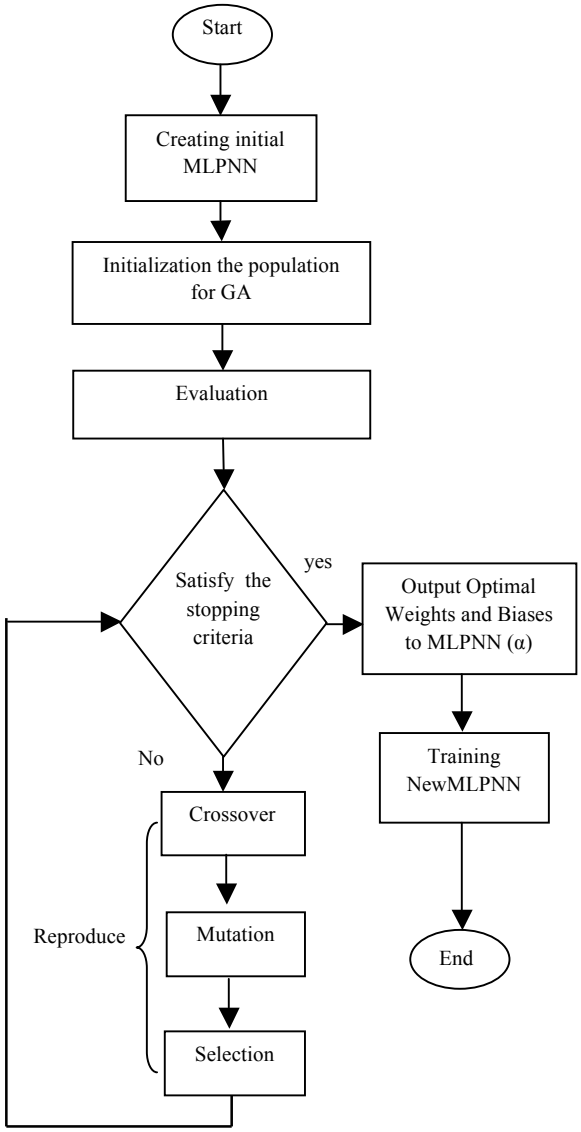

Fig .9. Flowchart optimization with GA algorithm

So, the error has a direct relationship with the weights to optimize.

$$E_{\Delta Vpv,\Delta Ppv} = \frac{1}{2}\left(desired - \frac{1}{1+e^{-\left(B_1+W_{1,10}\cdot\frac{1}{1+e^{-(B_{10}+W_{10,2}\cdot X_{\Delta Vpv,\Delta Ppv})}}\right)}}\right)^2 \quad (31)$$

$$E_{G,I_{PV}} = \frac{1}{2}\left(desired - \frac{1}{1+e^{-\left(B_1+W_{1,10}\cdot\frac{1}{1+e^{-(B_{10}+W_{10,2}\cdot XG,I_{PV})}}\right)}}\right)^2 \quad (32)$$

$$E_{G,I_{PV}} = \frac{1}{2}\left(desired - \frac{1}{1+e^{-\left(B_1+W_{1,10}\cdot\frac{1}{1+e^{-(B_{10}+W_{10,2}\cdot XG,I_{PV})}}\right)}}\right)^2 \quad (33)$$

The use of an ANN requires two stages. Firstly, the GA is used for establishing the initial values of the neural network weights as well as adapted it. Secondly, the neural network learns in a supervised process with couples of input vector and desired output.

3.2 Levenberg-Marquardt (LM) used to train Artificial Neural Network for PV MPPT system architectures.

The LM algorithm [15] has been evolved to resolve the problems of non-linear least squares. Is a standard algorithm for quadratic error optimization. LM is a method that combines two minimization approaches: the gradient descent approach and the Gauss-Newton approach. It behaves like a gradient descent approach when the parameters are not optimal, and behave like the Gauss-Newton approach when the set parameters are at optimal value. The principal reason for choosing the LM Algorithm resides on the size of the Hessian matrix [15] in terms of the amount of data in the learning database. Considering as an objective function the loss function which can be expressed as a number of errors squared in the form:

$$f = \sum e_{i,j}{}^2 = \sum \| e^2 \|, i = 1,2 \text{ and } j = 1,....,10 \quad [34]$$

$$e = \alpha_{desired} - \alpha_{optimised} \quad [35]$$

$$e_{i,j} = \alpha_{desired} - \frac{1}{1+e^{-\left(B_1{}^O + w_{110}{}^{HO}\cdot\frac{1}{1+e^{-\left(B_{10}{}^H + W_{210}{}^{IH}\cdot X_{\Delta V_{PV}.\Delta p_{PV}.}\right)}}\right)}} \quad [36]$$

With i: either the number of neurons in the input layer and in the output layer, j: the number of neurons in the hidden layer. As a function of error derivative with respect to the parameters, the Jacobian matrix of the loss function can be defined.

$$J_{i,j} f(w) = \frac{de_{i,j}}{dw_{i,j}} \quad [37]$$

Considering the Jacobian matrix size is m - n. we have:

$$\Delta f = 2J^T.e \quad [38]$$

With e being the vector that contains the errors terms. The Matrix of the Hessian [15] [19] is given by the expression:

$$Hf = 2J^T.\mathrm{J} + \lambda \mathrm{I} \quad [39]$$

The expression of LM which allows enhancing the parameters of the neural network in function to processes is defined as follows:

$$w_{i+1} = w_i - (\mathrm{J}_i{}^T \cdot \mathrm{J}_i + \lambda_i I)^{-1} \cdot (2J_i{}^T \cdot e_i), \mathrm{i}=0,1, \quad [40]$$

When $\lambda = 0$, in this case the Gauss-Newton method uses the Hessian matrix approximate, in the case of it is large it will become a gradient descent or error backpropagation with a low training rate. λ configuration is initialized for being large, such that the initial update was a small step in the gradient descent direction. On the other hand, if an iteration

results in a failure, λ is incremented with the help of a few factors. If not, as the loss is decreasing, λ decreases, such that that the LM algorithm approaches to the Newton method. Usually this process speeds up convergence at a minimum.

4. Results and Discussion

4.1. Simulation and experimentation testing context

In order to evaluate the effectiveness and the performance of the suggested MPPT monitoring techniques using optimization GAs with neural approaches, several tests have been performed for controlling the boost converter using Matlab/Simulink and implemented by DS1104 card. An experimental test bench inside the "IRIMAS" laboratory is designed with a hardware implimentation of a complete PV system composed of photovoltaic panel type 145W Solarex , a boost converter and a resistive load. chosen to facilitate the study like is shown in the fig (12). The proposed neural controllers GA are compared to the performance of a classical (P&O) control method using Matlab/Simulink and the best configuration is compared with the same structure using levenburg training algorithm and validated inside a real test bench using dspace 1104. As we are face on a non linear problem, from several tests and trials like is shown in table 1, in the hidden layer the neurons number was chosen to 10 in order to have a good trade-off between accuracy and calculation costs. The objectives of this work are to provide faster and more accurate MPP tracking under various climatic conditions, to predict PV output power and to eliminate fluctuations surrounding the MPP. Table 2 gives the simulation and experimental parameters system using in this application. From this purpose and based on both: standard profile (G=1000w/m^2, T=25°C), and real collected profiles, the following senarios are used to validate the robustness and efficiency related to our algorithms utilising Matlab/Simulink. Table 3 present an experimental GAs parameter's .

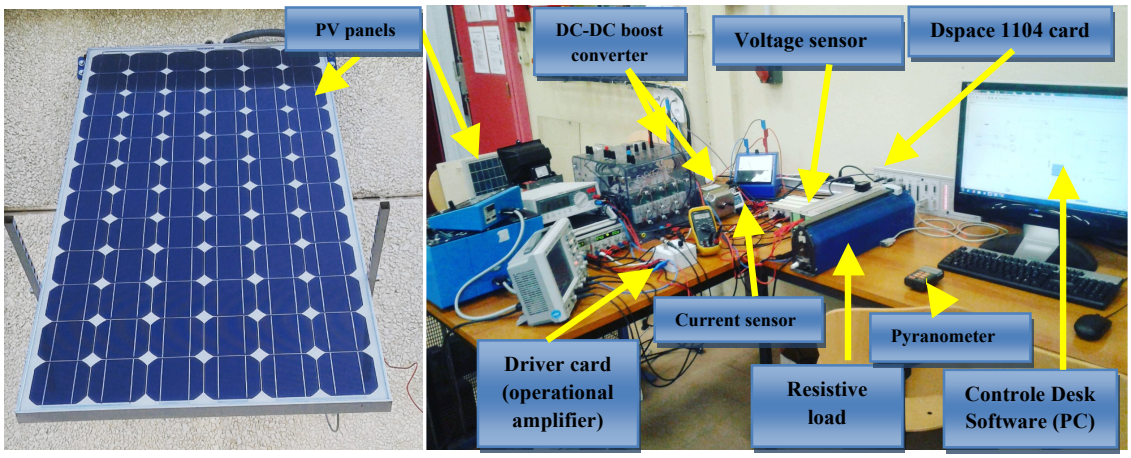

Fig. 12. Real time experimental test bench of PV solar conversion chain

Table 1: Performance comparisons of proposed MPPT methods

MPPT approach	P&O	GAANN1	GAANN2	GAANN3
Power fluctuations at steady-state	0.0155	$< 10^{-4}$	0.0194	$< 10^{-4}$
Efficiency ratio($100\times V_{Load}/V_{PV}$)	97.584%	97.599%	97.586%	97.655%
MSE in the case of nb of neuron 2-10-1	-	0.0311	0.0520	0.0079
MSE in the case of 2-50-1 neurons	-	0.0398	0.1040	0.1787
MSE in the case of 2-100-1 neurons	-	0.0597	1.1006	0.1369
nb of neurons in the input-hidden-output layers	-	2-10-1	2-10-1	2-10-1

nb of weights	-	41	41	41

system

Table 2. parameter's

Parameters	Simulation	experimental
DC- link capacitor of boost converter C_s (µF)	1100	2200
Inductor in the boost converter L (mH)	20	20
Switching Frequency (Khz)	10	10
Sampling time (µs)	10^{-4}	10^{-4}
Typical PV peak power (P_{mpp})	145W	145W
PV voltage at peak power (V_{mpp})	34.4 V	34.4 V
PV current at peak power (I_{mpp})	4.2A	4.2A
PV short-circuit current (I_{Sc})	4. 7A	4. 7A
PV open-circuit Voltage (V_{oc})	43.5V	43.5V

Table 3. Genetic algorithm parameter

Parameters	Value
Population size	50
Maximum power generation	500
Selection operator	0.85
Mutation operator, Pm	0.05
Crossover operator, Pc	0.9
Crossover type,	Two point by generation
Selection Type	Roulette wheel
Convergence time	47.803361s
Max generation	10

4.2. Normal conditions test (STC)

During this test, both temperature and irradiation were maintained constant. G=1000w/m^2, T=25°C. This simulation aims to establish the operating point offset from the MPP point. In addition, it is used to analyze wobble losses at this particular point. All three suggested P&O neuro-controllers are being compared to the traditional P&O controller. Results were shown in Fig. 15, in which (GAANN1) corresponds the first neuro-structure, that is to say the neural controller that uses GAs with only electrical measurements, (GAANN2) as a second neuro-structure, which uses GAs with both electrical / environmental measurement. (GAANN3) as a third structure, that is the neural controller that uses GAs with only environmental measurements. This figure shows the rapidity of the response provided by the 4 controllers. As we can see, GAANN1 and GAANN2 have a fast reponse with 0.05s while P&O and GAANN3 stabilisate only after 0.09s. At steady-state, the three GA-based neural controllers conserve the optimum voltage and current Vpv=34.4V and Ipv=4.26A. On the contrary, the conventional P&O is not able to conserve it. The duty cycle of the 4 controllers is presented by the Fig.15.d. The control P&O shows oscillations between 0.01% and 0.3%, GAANN2 control oscilate in the first time between 0.6 and 1 % to stabilisate quicly in 0.67 % in constrat GAANN1 control is stabilised in 0.65 %, and GAANN3 stabilised in 0.18 % additionally for each controller, Table 1 presents: the precise size of the power oscillations, the efficiency of the power conversion and the approach in terms of complexity. The efficiency of energy conversion is the relationship ratio between the effective power output delivered to the load and the power input obtained through the PV panel. Such a coefficient of efficiency is determined at the state of equilibrium (in permanent state). Always from the figure

15.d, both of the neural controllers that use electrical input parameters and environmental input parameters have a faster response time with smaller power fluctuations, compared to two other ones. These two controllers do not need a highest calculation costs, furthermore they are more efficient than the P&O approach.

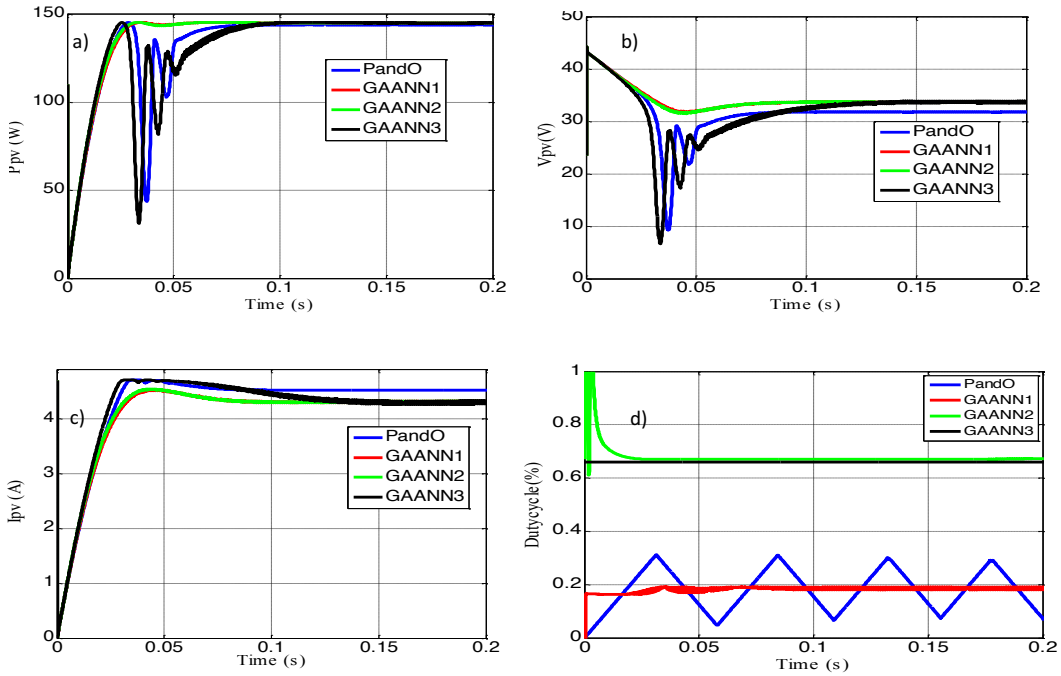

Fig. 15. a) PV module output power variation (P_{pv}) , b) PV module output voltage (V_{pv}), c) PV module output voltage (I_{pv}), d) duty cycle

4.3 Test under real changing conditions of temperature and irradiance

In the following scenarios, we specify two profiles evaluated at more realistic climatic conditions to validate the proposed neural GAs based MPPT controllers. The First one is an experimental profile based on real collected measures using environmental sensors collected at the IRIMAS laboratory over one complete day (17/11/2017). The solar radiation changes within a range of 315 W/m² to 750 W/m², and the corresponding temperature variation is in the range of 17.66°C to 20.7°C as it can be seen on Fig.16 a).The second one is a simulated smooth profile without perturbations over one day. The range of the variations of solar radiation is between 315 W/m² to 800 W/m² and the variations of the related temperature are between 17.66°C and 20.7°C. This is represented in Fig.17a). The duration of simulation for the two profiles is 1440 minutes, i.e., 1 measurement per minute over the 24h of the day.

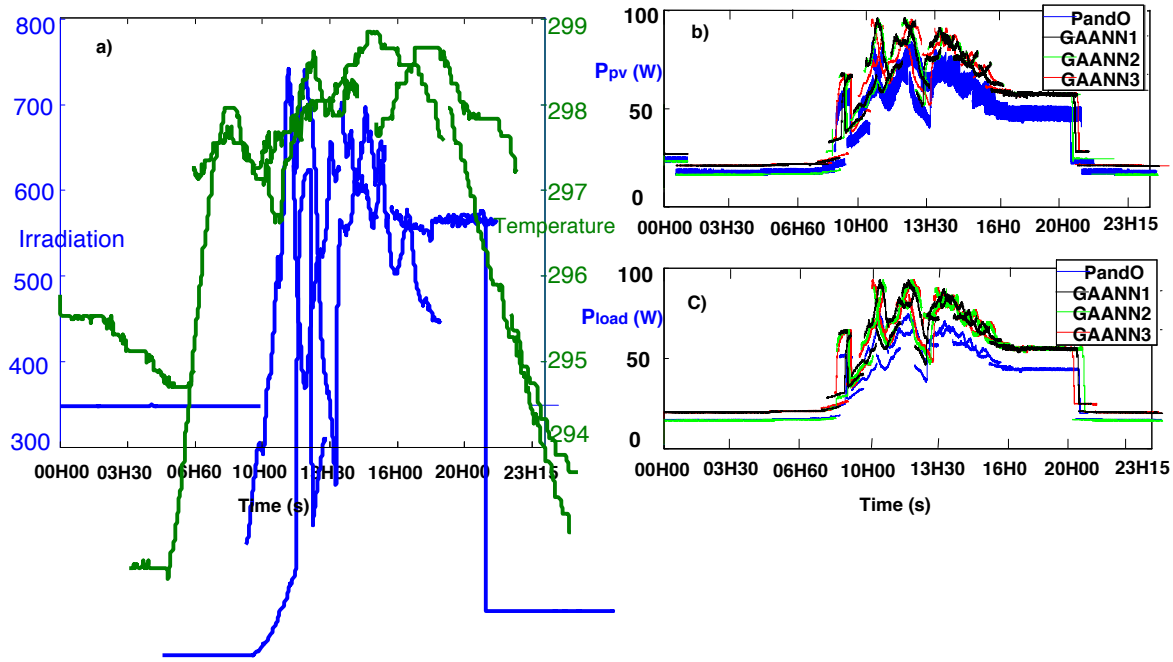

Fig. 16. a) Experimental real time profile collected at the IRIMAS laboratory b) Variations of module power at output PV panel using GA neural and P&O MPPT controllers c) Variations of module power at output load using GA neural and P&O MPPT controllers.

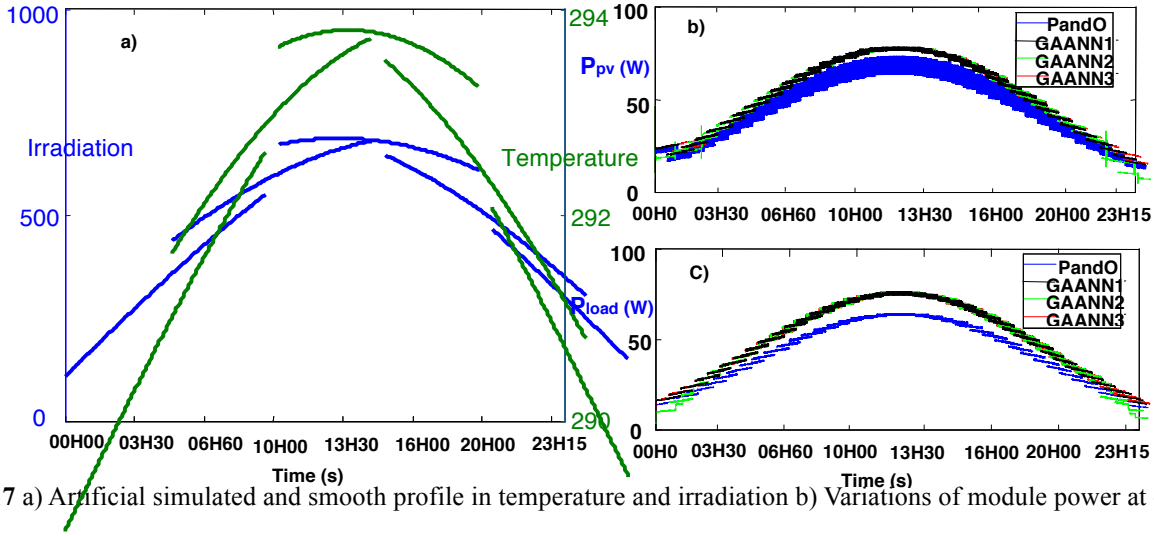

Fig.17 a) Artificial simulated and smooth profile in temperature and irradiation b) Variations of module power at output PV panel using GA neural and P&O MPPT controllers c) Variations of module power at output load using GA neural and P&O MPPT controllers.

The comparison of these results shows that the three GAs based neural controllers are faster, smooth and more able to maximize the more power extraction. However, the GAANN2 presents a drawback that consists in its inability to maximise the power when there is a low irradiation. This can be seen in Fig.16b), Fig.16c) between 00h00 and 07h30 where there is a power losses in comparing with GAANN1 and GAANN3 which have the benefit of being able to work in a fast and accurate manner without power losses. And this results are confirmed in Fig.17b) and Fig.17c). In contrast, the P&O controller has big drawbacks that consists in oscillations at MPP, late tracking capabilities and bad quality power extraction and big lost. Finally, the GA based neural controller that only uses electrical inputs GAANN1 and GAs based neural controller that only uses environmental inputs GAANN3 represents the best compromise between performances and computational costs.

4.4 Experimental tests

In this part a synopsis of the implementation of the MPPT tracking techniques using DS1104 acquisition card communicates between the system and a computer using the Matlab / Simulink and Control Desk software tools is shown in fig.18. By the help of the sensors, the output current and output voltage are measured in the terminals of the PV source as well as their derivative are calculated. These measurements are used by the proposed MPPT algorithm to generate a PWM signal to drive the boost converter. These measured signals have a lot of noise. They are filtered and adjusted in gain before sending them on the ADCs (Analogic Digital Converter) in the dSPACE board. More, a signal of 1 under Simulink is equivalent to ADC input or 10V DAC (Digital Analogic Converter) output, which justifies the use of gains of 10 (for ADCs) and 1/10 (for DACs) to offset the gains imposed by the dSPACE. This program is done in the real time interface diagram block of the PV system (RTI: Real Time Interface) programmed under the Matlab / Simulink environment. The implementation in real time is provided by a DS1104 card, a tool widely used in scientific research. From a computer, it is possible to program the input parameters of the system such as illumination and temperature. A control Desk software makes it possible to follow the evolution of the system; for example, the continuation of the PPM and even gives the possibility of modifying the parameters influencing the system.

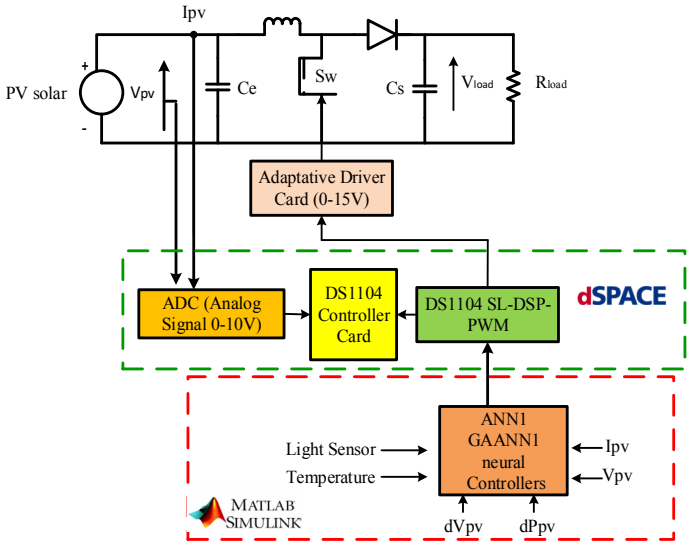

Fig. 18. Setup hardware implementation of solar conversion chain.

The real characteristics I-V, P-V of Solex PV panel is shown in the Fig.19 at a temperature of 25°C and irradiation of 780W/m^2, here the operating point far from the maximum power point (P_{pv} =114.7W, V_{pv}= 30.91V) because we aren't in the SMC, operating with a resistive load of (R≈30 ohm) out of control. From fig 20 to 23 two types of controllers are introduced: Electrical controller using GA as learning approach, represented by GAANN1 and electrical one using LM algorithm represented by ANN1. The resistive load is varied manually as it is shown in the fig.20 at a temperature of 21°C and irradiance of 600W/m^2. As a results both controllers present good behaviours: that are robustness without oscillations or power losses and present high accuracy. Meanwhile, the comparative study evince us the high-quality of the GAANN1, confirmed in real time by the good electrical performance of current, voltage and power in term of rapidity, precision and more power tracking giving by the figures 21, 22, 23. As well as the figures 24,a) 24,b) present respectively the experimental duty cycle of GAANN1 and ANN1. Figures 25 a ,b) and figures 26 a,b) present the experimental records by the Coray oscilloscope of V_{PV}, V_{load} and duty cycle for respectively GAANN1, ANN1. For the fig 25 the irradiance is reached 960 w/m^2 and the temperature not changed. As well as we keept varying the load. For the fig 26 we keept the load fixed. For this two last essays giving by the figures 25, 26) the irradiation is change randomly but approximatively the same, because we work with real PV panel and we can't control the real weather conditions.

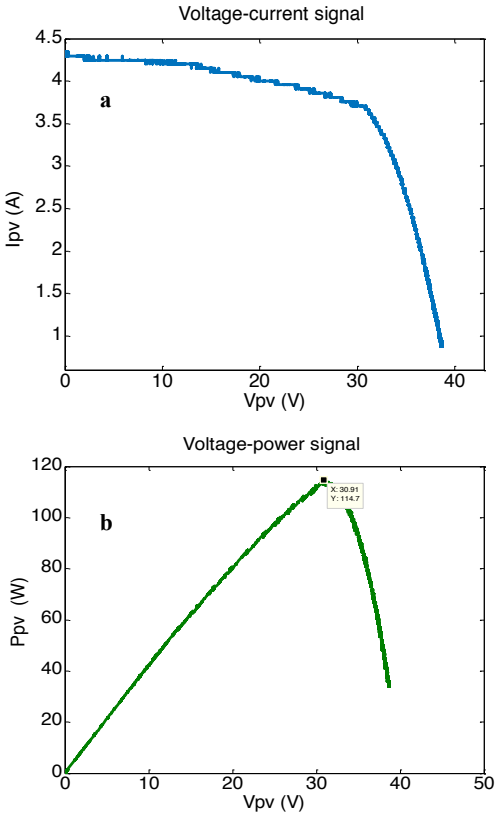

Fig. 19. Solarex PV measured characteristics a) voltage current signal.b) Voltage –power signal.

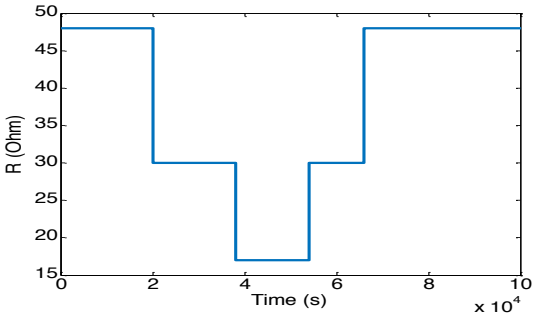

Fig. 20. Variable resistance

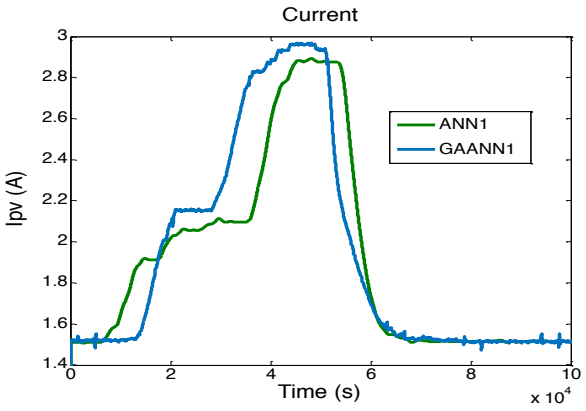

Fig. 21. Experimental PV output current

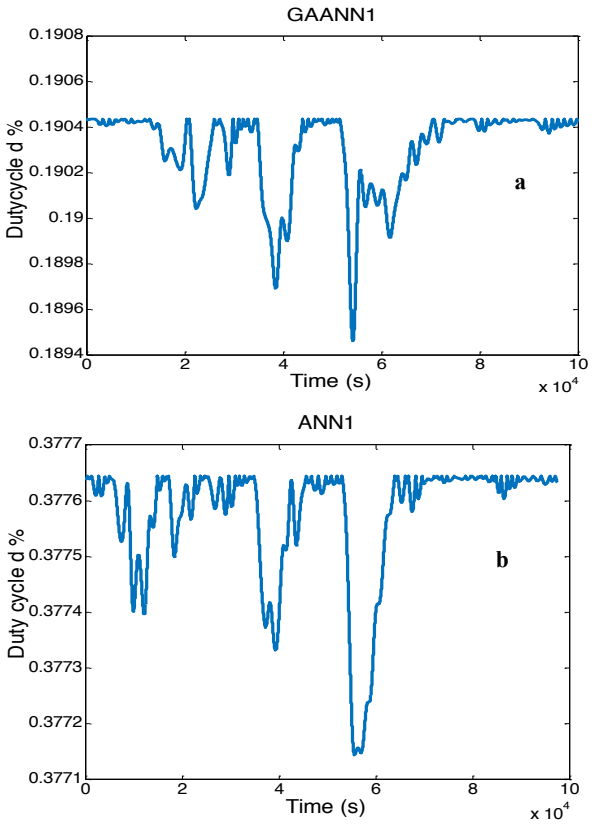

Fig. 24. Experimental duty cycle for a) GAANN1 b) ANN1

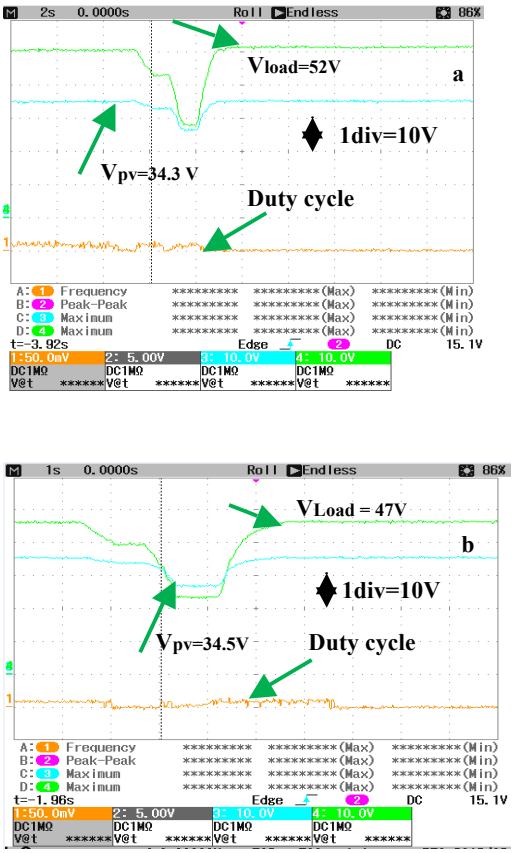

Fig .25. Experimental records by the Coray oscilloscope for a) GAANN1 b) ANN1.

Cost analysis of hardward setup :

Through this work we have developed a prototype of a medium-power / low-cost autonomous photovoltaic system that is cost-effective for remote areas. The aim is to minimize the cost of electricity production (€ or $/kWh) while ensuring optimal service continuity (reliability). The experimental tests presented in this section are based on a didactic IGBT converter "Semikron" multifunctional with frequency of f=25khz family "SEMISTACK - IGBT". This latter can operate as a DC-DC converter or as an AC-DC converter at the same time. Usable as a single-phase to three-phase converter, they can support a maximum voltage of 440 V on the AC side and 750 V on the DC side. The general idea in this realization is articulated on two important axes in order to optimize the cost and increase the efficiency of the installation:

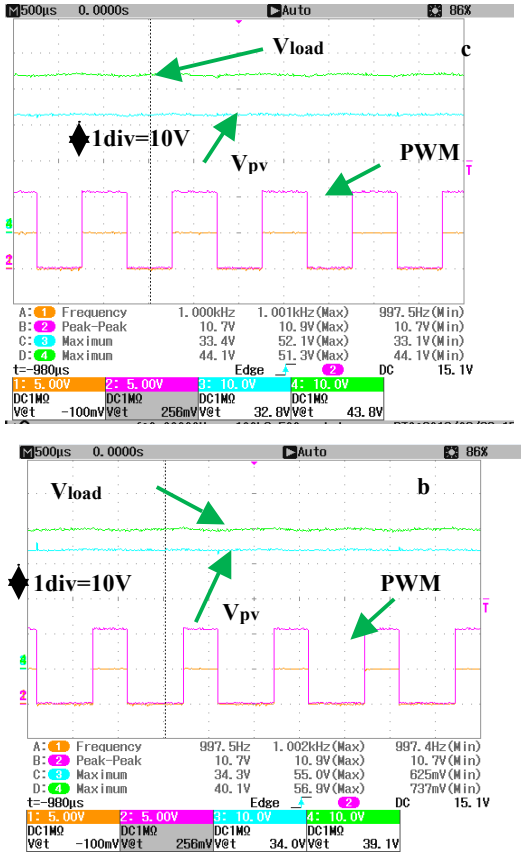

Fig. 26. Experimental records by the Coray oscilloscope at a fixed load for. c) GAANN1 d) ANN1.

-The dimensioning of the installation which is based on the choice of photovoltaic modules (costs of converters used, support structures, cables and installation result apart),

knowing that the end-user price for simple photovoltaic modules are now below 5 €/Wc. For this reason, a multifunctional high voltage converter was chosen that can be used as a boost for the MPPT and will then be used as an inverter to feed into the grid. In this case, diffrent margin photovoltaic generators can be connected to the complete system (low current, high voltage) which can support a voltage up to 750V, without involving a significant additional cost of wiring. As well as the converter will be adapted to the application to the system components (photovoltaic panels, loads...).

-The cost optimization is closely linked to the control strategy used. As we have seen through the comparison results, the controller implementation named GAANN1 was able to limit conversion losses and optimize energy management within the system compared to the other controller.

5. Conclusion

The main limits of conventional Maximum Power Point (MPP) tracking algorithms is that they present some oscillations in producing power and that they are not fast even under slow variations of weather conditions (temperature and solar radiation). To overcome these drawbacks, this article proposes to use more sophisticated controllers to rapidly track the MPP and to efficiently convert the power produced by a standalone PV panel. Neural network schemes have been designed for controlling a DC/DC boost converter working under changing conditions. These neural schemes are MLP optimized using a GA approach. After optimization and learning, they are able to model and to predict the PV output power only from measured data. Three GA based MLP structures are proposed with different inputs. The first one using only electrical measures, the second one using a mix between electrical and environmental input measures and the third structure relying only on environmental measures. The performance of the first electrical neural structure using GA learning approach in extracting the maximum power have been validated using Matlab/Simulink as a best solution, besides it is implemented inside on an experimental platform using dspace 1104 card with real PV Solarex panel, boost converter and resistive load. In addition is compared to the same structure using LM learning approach. As results the first proposed GA-based neural controller that take only electrical parameters in inputs track perfectly the MPP, as well as enhance energy supply efficiency conversion with a ratio of 97.599% .

References

[1] M. Seyedmahmoudian, A. Mohamadi, S,Kumary, A. Maung Than Oo, A. Stojcevski. “A Comparative Study on Procedure and State of the Art of Conventional Maximum Power Point Tracking Techniques for Photovoltaic System”, International Journal of Computer and Electrical Engineering, Vol.6, pp. 402-414. Septembre 2014.

[2] N. Kumar Elumalai, and A. Uddin, “Open circuit voltage of organic solar cells: an in-depth review”, Energy & Environmental Science, Vol.9, pp.391-410. 2016.

[3] A. Shazly. Mohammed, A.S. Montasir, “A comparative study of P&O and INC maximum power point tracking techniques for grid-connected PV systems”, SN Applied Sciences, Vol.1, pp.11-13. January 2019.

[4] R. Ahmad, Ali F. Murtaza, H. A. Sher, “Power tracking techniques for efficient operation of photovoltaic array in solar applications – A review”, Renewable and Sustainable Energy Reviews, Vol.101, pp.82-102. March 2019.

[5] J. Lakhmi, and N.M. Martin, Fusion of Neural Networks, Fuzzy Systems and Genetic Algorithms, 1st ed., New York Washington: CRC Press LLC, Press, 1998, pp.1-367.

[6] P. Sen, P. R. Bana, K. P. Panda, “Firefly Assisted Genetic Algorithm for Selective Harmonic Elimination in PV Interfacing Reduced Switch Multilevel Inverter”, International Journal of Renewable Energy Research Vol.9, pp.1-10. 2019.

[7] C.M. Bishop, Neural Networks for Pattern Recognition, Oxford University Press, Inc. New York, NY, USA: Clarendon Press, 1995, pp.1-498.

[8] M. Karel, “Impact of photovoltaics on frequency stability of power system during solar eclipse”, IEEE Transactions on Power System, Vol.31, pp.3648-3655. March 2016.

[9] J.D. Tang, Chenweiand H. Guang-Bin, “ Extreme Learning Machine for Multilayer Perceptron”, IEEE Transactions on Neural Networks and Learning Systems, Vol.07, pp.809-821, May 2015.

[10] F.Lukas, and M. Dusan. “Financial Time Series Modelling with Hybrid Model Based on Customized RBF Neural Network Combined With Genetic Algorithm”, Advances in electrical and electronic engineering, vol. 12, pp. 307-318, december 2014.

[11] M. Tanaka, H. Eto, Y, Mizuno, N. Matsui, F. Kurokawa “Genetic algorithm based optimization for configuration and operation of emergency generators in medical facility” IEEE 6th International Conference on Renewable Energy Research and Applications (ICRERA), USA, pp.919-924, November 2018.

[12] S. Dezs″o, “Real-time Modelling, Diagnostics and Optimised MPPT for Residential PV Systems“,Institut for Energiteknik, Aalborg University, 2009. (Ph.D. dissertation,).

[13] K.N.Shukla, R. Saroj, and K. Sudhakar. “Mathematical

modelling and experimental validation of characteristics of amourfous (A-SI) and polycrystalline (P-SI) solar PV modules", 1st National Convention of Electrical Engineers & National Seminar on Renewable Energy and Green Technology for Sustainable Development At: Bhopal (conference), India, pp.1-27, October 2015.

[14] C . Özgür, and A. Teke. "A Hybrid MPPT method for grid connected photovoltaic systems under rapidly changing atmospheric and Technology", Electric Power Systems Research, Vol. 152, pp. 194-210. November 2017.

[15] S- a. Blaifi, S. Moulahoum, B. Taghezouit, A. Saimd, " An enhanced dynamic modeling of PV module using Levenberg-Marquardt algorithm", Renewable Energy, Vol. 152, pp. 745-760. May 2019.

[16] A. H. Elsheikh, S. W. Sharshir, M. Abd Elaziz A.E.Kabeel, W. Guilang , Z. Haiou, " Modeling of solar energy systems using artificial neural network: A comprehensive review", Vol. 180, pp. 622-639. March 2019.

[17] I. Chtouki, P.Wira, and M. Zazi. "Comparison of several neural network perturb and observe MPPT methods for photovoltaic applications", IEEE 19th International Conference on Industrial Technology (ICIT), lion, France, pp.1-6, 30 April 2018.

[18] M.Habib, F. Khoucha and A.Harrag. " GA-based robust LQR controller for interleaved boost DC–DC converter improving fuel cell voltage regulation ", Electric Power Systems Research, Vol. 3, pp. 438–456. Novembre 2017.